Published in final edited form as:
Cell. 2007 December 28; 131(7): 1327–1339. doi:10.1016/j.cell.2007.11.039.

STIM2 is a Feedback Regulator that Stabilizes Basal Cytosolic and Endoplasmic Reticulum Ca^{2+} Levels

Onn Brandman*, **Jen Liou**, **Wei Sun Park**, and **Tobias Meyer***
Department of Chemical and Systems Biology, Bio-X/Clark Center W200, Stanford University, Stanford, CA 94305

Summary

Deviations in basal Ca^{2+} from normal levels interfere with receptor-mediated Ca^{2+} signaling as well as endoplasmic reticulum (ER) and mitochondrial function. While defective basal Ca^{2+} regulation has been linked to various diseases, the regulatory mechanism that controls basal Ca^{2+} is poorly understood. Here we performed a siRNA screen of the human signaling proteome to identify regulators of basal Ca^{2+} concentration and found STIM2 as the strongest positive regulator. In contrast to STIM1, a recently discovered signal transducer that triggers Ca^{2+}-influx in response to receptor-mediated depletion of ER Ca^{2+} stores, STIM2 activated Ca^{2+} influx upon smaller decreases in ER Ca^{2+}. STIM2, like STIM1, caused basal Ca^{2+} influx via activation of the plasma membrane Ca^{2+} channel Orai1. Our study places STIM2 at the center of a feedback module that keeps basal cytosolic and ER Ca^{2+} concentrations within tight limits.

Introduction

Ca^{2+} is a ubiquitous second messenger that regulates secretion, contraction, gene expression and other cell functions. In unstimulated cells, the basal cytosolic concentration of Ca^{2+} is kept constant at a concentration ~10,000 fold below the extracellular and endoplasmic reticulum (ER) Ca2+ concentration (Berridge et al., 2003). Receptor stimuli typically increase Ca^{2+} concentration up to ten-fold from basal by opening Ca^{2+} channels in the plasma membrane (PM) or ER membrane. These Ca^{2+} signals are generated by a dynamic system that relies on Ca^{2+} channels and pumps in the PM and ER (Figure 1A).

Tremendous progress has been made in recent years in understanding how receptor stimuli regulate different Ca^{2+}-channels. However, less is known about regulatory feedback mechanisms that maintain a constant basal Ca^{2+} concentration. The importance of tight control of basal Ca^{2+} concentration is indicated by numerous diseases that have been associated with prolonged increases or decreases in basal Ca^{2+} concentration. For example, cells derived from Alzheimer patients with genetic mutations in presenilin have defects in Ca^{2+} homeostasis due to changes in the rate of basal Ca^{2+}-flux out of the ER Ca^{2+} store (Tu et al., 2006). Changes in basal Ca^{2+} homeostasis have also been associated with diseases and conditions such as endothelial dysfunction (Shulman et al., 2005), kidney disease (Thebault et al., 2006), cardiac dysfunction (Ter Keurs and Boyden, 2007), Huntington disease (Bezprozvanny and Hayden,

*Corresponding authors: Onn Brandman E-mail: onn@stanford.edu, Tobias Meyer E-mail: tobias1@stanford.edu.

2004), as well as other neurodegenerative and aging related diseases (Treves et al., 2005; Raza et al., 2007).

Mechanistically, these different disease states and conditions are believed to be caused by long-term increases or decreases in basal Ca^{2+} concentration that then result in defective Ca^{2+} signaling (Ter Keurs and Boyden, 2007), reduced ER Ca^{2+} concentration and ER stress (Zhang & Kaufman, 2006) or mitochondrial dysfunction (Campanella et al., 2004). Long term changes in basal Ca^{2+} also alter protein degradation (Spira et al., 2001) and transcription (Gallo, 2006) which may indirectly interfere with cell health.

The active components that maintain Ca^{2+} gradients in human cells are believed to be four different PM pump isoforms (PMCAs) (Strehler et al., 2007; Guerini et al., 2005) and three PM Ca^{2+} transporters (Na^{+}/Ca^{2+}-exchangers) (Philipson et al., 2002) as well as three different ER Ca^{2+} pump isoforms (SERCAs) (Periasamy, 2007). Less is known about the nature of basal Ca^{2+} influxes to the cytosol from outside of the cell and from ER Ca^{2+} stores, but some Ca^{2+} channels and other Ca^{2+} leak activities have been proposed to play a role (Tu et al., 2006; Pinton and Rizzuto, 2005; Camello et al., 2002). Remarkably, many researchers have observed that basal Ca^{2+} levels in cells change little in response to large changes in extracellular Ca^{2+} concentration, arguing that a highly effective feedback control exists to stabilize basal Ca^{2+} concentration (Kusters et al., 2005).

We set out to pursue a siRNA screening strategy to learn more about feedback mechanisms that ensure that basal Ca^{2+} levels are kept within narrow limits in cells. We used two sensitized screening conditions and live single cell Ca^{2+} imaging to enhance our ability to identify possible regulators. Since we were interested in signaling proteins, we made use of a Dicer-generated siRNA library of the human signaling proteome that we had previously generated (Liou et al., 2005). In addition to the expected findings that knocking down known Ca^{2+} pumps or calmodulin increase basal Ca^{2+} concentration, we found that knocking down STIM2 had the strongest effect on reducing basal Ca^{2+} concentration. We observed that over-expression of STIM2 but not its homolog STIM1 markedly enhanced basal Ca^{2+} concentration by regulating the plasma membrane Ca^{2+}-channel Orai1. We also found that, upon Ca^{2+} store depletion, a YFP-STIM2 construct showed dynamic translocation from a uniform ER distribution to ER-PM junctions similar to the behavior of STIM1 (Liou et al., 2005). However, unlike the translocation of STIM1, STIM2 was able to translocate to ER-PM junctions with only small decreases in ER Ca^{2+} concentration, explaining why STIM2 but not STIM1 serves as a regulator of basal Ca^{2+}.

Results

Design of a sensitized siRNA screen to identify regulators of basal Ca^{2+} concentration

We developed a siRNA screening protocol to identify human genes that regulate basal cytosolic Ca^{2+} concentration. HeLa cells were sensitized by subjecting their Ca^{2+} signaling system to two opposing pressures: 24 hours in *high* extracellular Ca^{2+} (+10 mM) and, in a separate experiment, 24 hours in *low* extracelluar Ca^{2+} (~0.1 mM). This strategy was devised to push the Ca^{2+} homeostatic control system towards its limits so that the effect of the RNAi perturbations could be more readily observed. We used the ratiometric Ca^{2+} indicator Fura-2 (Grynkiewicz et al., 1985) and an automated fluorescence imaging system to measure siRNA-mediated differences in basal Ca^{2+} concentration. An approximately 5 nM reduction was caused by the low and 2.5 nM increase by the high Ca^{2+} condition from a basal level of ~ 50 nM. Approximately 1000 individual cells in each well of a 384-well plate were analyzed and the mean single cell Fura-2 ratio was computed for each well (Figure 1B).

We tested the usefulness of our strategy by making a Dicer-generated Ca^{2+} siRNA set that included known and putative Ca^{2+} pumps, channels and exchangers (Figure 1C; Table S1 for a list of results). The strongest hit in the high external Ca^{2+} condition was the plasma membrane Ca^{2+}-ATPase PMCA1. This is consistent with a role of plasma membrane Ca^{2+} pumps as a main avenue for Ca^{2+} extrusion out of these cells (Guerini et al., 2005). The strongest hit in the low external Ca^{2+} condition was the endoplasmic-reticulum Ca^{2+} pump SERCA2, which transports Ca^{2+} from the cytosol into the ER (Strehler et al., 2007). This effect was also expected since thapsigargin, an inhibitor of SERCA pumps, is known to trigger persistent increases in cytosolic Ca^{2+} concentration (Thastrup, 1990). These test measurements demonstrated that our assay system is able to identify different types of regulators of basal Ca^{2+} concentration.

Identification of STIM2 as a primary regulator of basal Ca^{2+} concentration

We then screened the Dicer-generated siRNA library targeting the human signaling proteome. 2304 signaling gene products were individually knocked down in duplicate for both the high and low external Ca^{2+} conditions. From this initial screen, we selected statistically significant positive and negative regulators of basal Ca^{2+} concentration and remade Dicer-generated siRNA constructs for the top 112 putative hits. We then re-screened these siRNAs in triplicate and found that the siRNAs targeting STIM2 and calmodulin 1 (Calm1) were the strongest positive and negative regulators, respectively (Figure 1D). Table S2 lists the statistically significant results from these two high and low Ca^{2+} screens.

Consistent with the known function of calmodulin to bind and activate PM Ca^{2+} pumps, Calm1 knockdown had a similar relative effect as PMCA1 knockdown for both sensitized conditions. Surprisingly, however, the STIM2 gene product was the number one hit in the *low* Ca^{2+}_{ext} condition. We were particularly intrigued by this finding since STIM2 shares 47% homology to the recently identified ER-Ca^{2+} sensor STIM1 which functions at the center of a signaling pathway that links receptor-mediated release of ER Ca^{2+} to the opening of plasma membrane Ca^{2+} channels (Roos et al., 2005; Liou et al., 2005). STIM2 is a multi-domain transmembrane protein that is at least partially localized to the ER, interfacing both the lumen of the ER and the cytosol (Figure 1E) (Liou et al., 2005; Dziadek and Johnstone, 2007). Conflicting results have been reported about a possible role of STIM2 in negatively regulating STIM1 (Soboloff et al., 2006a) or positively regulating store-operated Ca^{2+} influx (Liou et al., 2005; Soboloff et al., 2006b). We focused our subsequent studies on the role of STIM2 in regulating basal Ca^{2+} homeostasis.

STIM2 knockdown selectively lowers basal cytosolic and ER Ca^{2+} concentrations

We used synthetic STIM2 siRNA to investigate the effect of STIM2 knockdown on basal Ca^{2+} concentration under normal external Ca^{2+} concentrations (1.5 mM). We also compared the effect of a knockdown of STIM2 to that of its isoform STIM1. Consistent with a unique role of STIM2 in regulating basal Ca^{2+}, STIM2 knockdown, but not STIM1 knockdown, significantly lowered basal cytosolic Ca^{2+} in HeLa, HUVEC and HEK293T cells (Figure 2A). STIM1 and STIM2 knockdowns were effective and isoform-specific when assayed by Western blot (Figure 2B) in HeLa cells.

We also determined the consequence of STIM2 or STIM1 knockdown on the basal Ca^{2+} level in ER stores. We tested ER Ca^{2+} levels first by addition of the membrane permeant Ca^{2+} ionophore ionomycin together with external application of the Ca^{2+} chelator EGTA and by quantifying the induced cytosolic Ca^{2+} peak (Figure 2C). Ionomycin is known to rapidly release Ca^{2+} from internal Ca^{2+} stores and external EGTA was included to prevent Ca^{2+} influx from outside the cell. Since the ER is the primary Ca^{2+} store in the cell, it is therefore expected that the measured relative amplitude of the induced Ca^{2+} peak (Δpeak Ca^{2+}) directly reflects

the loading level of ER Ca^{2+} stores (full traces are shown in Figure S1). Using this approach, STIM2 knockdown led to a marked decrease in ER Ca^{2+} levels while STIM1 knockdown had a smaller effect.

In a second approach, we transfected HeLa cells with the ER targeted Ca^{2+} indicator D1ER (Palmer et al., 2004). Only siSTIM2 treated cells showed a significant decrease in ER Ca^{2+} as measured by the relative decrease in the ER FRET signal (Figure 2C). Thus, knockdown of STIM2 reduces both basal cytosolic as well as basal ER Ca^{2+} concentrations.

The effect of PMCA1, SERCA2, and STIM2 knockdowns on basal cytosolic Ca^{2+} levels can be parsimoniously explained by a simple model relating the extracellular, cytosolic, and ER Ca^{2+} pools (Figure 2D). In unstimulated cells with intact pumps and channels, long-term changes in cytosolic Ca^{2+} concentration are expected to be paralleled by changes in ER Ca^{2+} concentration. PMCA knockdown attenuates export of Ca^{2+} from the cell and would therefore result in an increase in cytosolic as well as ER Ca^{2+} concentrations. SERCA knockdown lowers ER Ca^{2+} levels, thereby activating store-operated Ca^{2+} influx which increases cytosolic Ca^{2+} concentration. In contrast, the finding that STIM2 knockdown lowers Ca^{2+} concentration both in the cytosol and ER suggests that it has a role as a positive regulator of basal Ca^{2+}-influx that increases cytosolic Ca2+ concentration as well as ER Ca2+ concentration.

STIM2 and STIM1 have distinct roles in regulating basal Ca^{2+} influx versus receptor triggered store-operated Ca^{2+} influx

We next used over-expression of YFP-STIM1 and YFP-STIM2 fusion proteins to better understand the roles of the two isoforms. We used automated low magnification imaging to measure Ca^{2+} concentration together with the relative concentration of expressed YFP-STIM1 or YFP-STIM2 in thousands of individual cells. The YFP intensities were normalized using the autofluorescence of untransfected cells as a reference and we then grouped all the cells according to STIM expression. The cell-to-cell variability of expression levels guaranteed that we covered the full range of STIM expression in each experiment. Using this analysis, transient expression (9 hour) of YFP-STIM2 or YFP-STIM1 both increased basal Ca^{2+} as a function of the expression level. However, expression of YFP-STIM2 increased basal Ca^{2+} levels much more than expression of the same concentration of YFP-STIM1 (Figure 2E). Expression of YFP alone is shown as a control. This provides further support for a primary role of STIM2 but not of STIM1 in regulating basal Ca^{2+} concentration.

We then measured store operated Ca^{2+}-influx (SOC) using Ca^{2+} add back experiments in cells where Ca^{2+} stores had been maximally depleted by thapsigargin in low external Ca^{2+}. Expression of STIM2 increased Ca^{2+} influx, albeit less than expression of the same concentration of STIM1 (Figure 2F). This argues that both STIM1 and STIM2 can sense the depletion of ER Ca^{2+} levels and can trigger plasma membrane Ca^{2+} influx. As a control, expression of a STIM2 construct without a protein tag also increased Ca^{2+}-influx after ER store depletion (Figure S2). This led to our working model that STIM2 serves as the primary regulator for basal Ca^{2+}-influx while STIM1 and STIM2 both trigger Ca^{2+} influx following receptor-mediated ER store-depletion.

ER Ca^{2+} store depletion triggers STIM2 translocation to ER-PM junctions

We used the YFP conjugated STIM2 construct to investigate whether it undergoes store-depletion triggered translocation as was shown previously for STIM1 (Liou et al., 2005). Strikingly, YFP-STIM2 was initially mostly distributed across the ER, and thapsigargin-induced ER Ca^{2+} store depletion led to a rapid translocation of YFP-STIM2 to PM localized puncta (Figure 3A). We observed the same YFP-STIM2 puncta formation in HeLa, HUVEC,

and HEK293T cell lines (Figures 3A–C). To minimize expression artifacts, only cells with a low range of YFP-STIM2 expression are shown in these panels.

We next compared STIM1 and STIM2 localization by co-transfection of CFP-STIM1 and YFP-STIM2 followed by thapsigargin-induced depletion of ER Ca^{2+} stores. CFP-STIM1 and YFP-STIM2 were co-localized in the same puncta that have previously been characterized as ER-PM junction sites (Figure 3D) (Liou et al., 2005, Wu et al., 2006). Finally, we tested whether the punctate localization of STIM2 is driven by Ca^{2+} dissociation from its EF-hand by creating an EF-hand mutant of STIM2 that disrupts the EF-hand Ca^{2+} binding site (Asp 80 to Ala). The STIM2 EF-hand mutant ($STIM2_{EF}$) was prelocalized to ER-PM junctions and did not significantly change distribution in response to thapsigargin (Figure 3E). This argues that STIM1 and STIM2 make use of a common regulatory mechanism that involves Ca^{2+} dissociation, oligomerization and translocation in order to signal from the lumen of the ER to the ER-PM junction sites (Liou et al., 2007). In order to facilitate the discussion of the distinguishing features of basal versus receptor-triggered Ca^{2+}-influx, we refer to them in the text below as B-SOC and R-SOC, respectively.

Given the similarities in the observed STIM1 and STIM2 activation mechanism, we tested whether the effect of STIM2 on B-SOC is mediated by the PM Ca^{2+} channels Orai1, 2 or 3, as has been shown for R-SOC in the case of STIM1 (Feske et al., 2006; Peinelt et al. 2006; Luik et al., 2006; Yeromin et al., 2006; Mercer et al., 2006). We expressed STIM2 in cells pre-treated with siRNA targeting Orai1, Orai2, or Orai3 using isoform specific siRNAs. Orai1 knockdown abrogated the effect of STIM2 expression on basal Ca^{2+} by more than 80% (Figure 3F) while targeting of Orai2 or Orai3 had a smaller effect. This argues that HeLa cells make use of Orai1 Ca^{2+} channels for B-SOC as well as R-SOC Ca^{2+} influx. We note that in cells without STIM2 expression, knockdown of Orai isoforms lowered basal Ca^{2+} to a lesser extent compared to the knockdown of STIM2 (Figure S3). This lower suppression may be caused by insufficient knockdown, additive contributions from different Orai-isoforms or from other channels regulated by STIM2.

Translocation of STIM2 but not STIM1 in response to small reductions in ER Ca^{2+} concentration

Our imaging and functional studies suggest that key features of the molecular regulation of STIM2 and STIM1 are the same. A plausible mechanism explaining why they differentially regulate basal Ca^{2+} is a different sensitivity of STIM1 and STIM2 to ER Ca^{2+} concentration. STIM2 may already be partially active at basal ER Ca^{2+} concentrations and become more active by small reductions in ER Ca^{2+}, while STIM1 may require much larger receptor-triggered reductions in ER Ca^{2+} to be activated.

To test this hypothesis, HeLa cells were cotransfected with CFP-STIM1 and YFP-STIM2 and then subjected to slow ER Ca^{2+} store depletion by removing external Ca2+ using EGTA addition. Strikingly, YFP-STIM2 started to form puncta at ER-PM junctions before CFP-STIM1 following external EGTA addition (Figure 4A). While the time to reach half-maximal puncta for YFP-STIM2 was ~= 10 minutes, CFP-STIM1 puncta formation was half-maximal after only ~= 30 minutes (Figure 4A–B). When ER stores were depleted by thapsigargin, STIM2 formed puncta more rapidly, but again before STIM1 (Figure S4). The slower rate in STIM1 puncta formation is not due an intrinsic delay of the translocation process, since STIM1 puncta form within less than 1 minute upon rapid Ca^{2+} store depletion by ionomycin (Liou et al., 2005). These experiments strongly suggest that STIM2 is activated at higher ER Ca^{2+} concentrations and therefore will translocate to ER-PM junctions and activate Ca^{2+} influx even for small reductions in ER Ca^{2+} levels. In contrast, STIM1 requires a larger reduction in ER Ca^{2+} to be activated.

In order to determine the ER Ca^{2+} levels and the degree of cooperativity for translocation of STIM1 and STIM2, we used ionomycin triggered Ca^{2+} release to estimate the remaining Ca^{2+} in ER stores at different time points after EGTA addition. Alternatively, we measured the same time constant using the ER Ca^{2+} probe D1ER (Figure S5). Assuming that the basal ER Ca^{2+} concentration is approximately 400 μM (300–500 μM values derived in the literature: Brini et al., 1999; Yu and Hinkle, 2000; Montero et al., 2001), we plotted the degree of STIM1 and STIM2 translocation as a function of ER Ca^{2+} levels (Figure 4C) and fit the ER Ca^{2+} dependence of translocation to a cooperative activation model. Since the observed puncta formation has been shown to involve sequential Ca^{2+} dissociation, oligomerization, and translocation steps (Liou et al., 2007), our STIM activation model computes an overall cooperativity of the multi-step process (Figure 4C):

$$\text{STIM Puncta} = \alpha - \beta * {Ca^{2+}}_{ER}{}^{N} / ({Ca^{2+}}_{ER}{}^{N} + {EC_{50}}^{N})$$

Where N is the cooperativity of the overall process, EC_{50} is the Ca^{2+} concentration for half-maximal translocation and α and β are normalization constants.

A best fit of this model was obtained with EC_{50} for STIM2 and STIM1 of 406 and 210 μM, respectively, and N = 5 and 8 for the cooperativity of STIM2 and STIM1, respectively (α=0.91, β=0.83 for STIM1; α= 0.84, β=1.5 for STIM2). This is consistent with a two-fold lower Ca^{2+} sensitivity of STIM2 compared to STIM1. An important finding from this analysis was that STIM1 translocation is regulated with high cooperativity in relation to the ER Ca^{2+} concentration. This high cooperativity, combined with its higher affinity for Ca^{2+}, can explain how STIM1 is kept effectively inactive at basal ER Ca^{2+} concentrations.

Since this analysis predicts that STIM2 is partially active at basal conditions, we tested whether overloading the ER would reduce STIM2 puncta to levels below basal. We used the reversible SERCA inhibitor 2′,5′-di(tert-butyl)-1,4-benzohydroquinone (BHQ) followed by addition of 10 mM Ca^{2+} extracellular buffer to briefly hyperload the ER. As predicted, BHQ+EGTA caused STIM2 distribution to become more punctate in response to the lower ER Ca^{2+} (Figure 4D), and the subsequent addition of high extracelluar Ca^{2+} triggered a near complete loss of observable STIM2 puncta below the basal level. This result is consistent with STIM2 being partially punctate and active at basal conditions.

STIM2 but not STIM1 effectively activate Ca^{2+}-influx in a partial Ca^{2+} store-depletion protocol

We also tested for different Ca^{2+} sensitivities of STIM1 and STIM2 by using the reduced ER Ca^{2+} loading protocol described in Figure 1 for the sensitized screen (0.1 mM external Ca^{2+}). Cytosolic Ca^{2+} levels were compared as a function of YFP-STIM1 or YFP-STIM2 expression levels for normal as well as reduced ER loading (Figure 4E–F). We used mutant STIM proteins that cannot bind Ca^{2+} (constitutively active EF-hand mutants) as a reference and compared them to wildtype STIM proteins that can be inhibited by ER Ca^{2+}.

Expression of increasing levels of EF-hand mutants of STIM1 or STIM2 triggered relative Ca^{2+} increases that were, as expected, insensitive as to whether we measured under normal or reduced ER loading conditions (Figure 4E–F). Also, as expected, for the condition of normal ER Ca^{2+}, wildtype STIM1 and STIM2 were less potent in raising Ca^{2+} than their EF-hand mutant counterparts, albeit STIM2 was much more potent than STIM1 (Figure 4E–F). This is consistent with a strong inhibition of STIM1 and a weaker inhibition of STIM2 by normal ER Ca^{2+} levels. This differential regulation becomes even more clear for the measurements at the partially reduced ER Ca^{2+} concentration where STIM2 becomes nearly as potent as its EF-hand mutant in raising Ca^{2+}, indicating that Ca^{2+} had almost completely dissociated from STIM2 (Figure 4E). STIM1, by contrast, was still much less effective compared to the STIM1

EF-hand mutant, suggesting that it was still mostly inhibited by Ca^{2+} (Figure 4F) (Non-normalized data is presented in Figure S6). This functional comparison provides additional evidence that STIM2 selectively activates Ca^{2+} influx for normal and partially depleted ER Ca^{2+} conditions for which STIM1 mediated Ca^{2+} influx is effectively suppressed.

Since these results pointed to possible differences in the EF hand Ca^{2+} binding affinity of STIM1 versus STIM2, we exchanged the three key sites that are different between the EF hands of STIM1 and STIM2 (positions 79,80,82 in STIM1 and 83,84,86 in STIM2). If the EF hand domain alone were responsible for the difference in sensitivity, the effect of expression of $STIM1_{EF->STIM2}$ should be the same as that of STIM2 and vice-versa for the $STIM2_{EF->STIM1}$ construct. Indeed, expression of $STIM1_{EF->STIM2}$ produced a construct with a higher Ca^{2+} sensitivity similar to that of STIM2 (Figure S7) that still senses ER calcium levels (Figure S6). Nevertheless, expression of $STIM2_{EF->STIM1}$ did not exhibit STIM1-like properties (data not shown). This argues that the activation threshold for STIM1 and STIM2 is in part regulated by the three amino acid difference in the EF hand region but must involve in addition other parts of the two proteins.

STIM2-regulation of Ca^{2+}-influx does not require STIM1

Since STIM1 and STIM2 have been shown to be able to form hetero-oligomers (Dziadek and Johnstone, 2007; Stathopulos, 2006), it is plausible that they function as a complex and that STIM2 requires STIM1 to signal to Orai1 channels for both B-SOC and R-SOC type Ca^{2+} influx. We used over-expression of STIM2 combined with STIM1 knockdown to test for such a possible co-regulation. Figure 5A shows that STIM1 knockdown did not significantly alter the increase in basal Ca^{2+} resulting from STIM2 expression. Furthermore, STIM1 knockdown also did not interfere with the ability of YFP-STIM2 expression to enhance store-depletion-triggered Ca^{2+}-influx (Figure 5B). For comparison, knockdown of Orai1 markedly suppressed the ability of expressed STIM2 to enhance store-operated Ca^{2+} influx. A reciprocal control experiment with the same result is shown in Figure 5C. This demonstrates that each of the two STIM isoforms can regulate Orai1 in the absence of the other.

While working with cells that overexpress YFP-STIM2, we noticed that longer expression (24 hours instead of 9 hours) led to a significant reduction in the maximal attainable store-operated Ca^{2+} influx (Figure 5D,E). This indicates that a slow adaptive mechanism downregulates store-operated Ca^{2+} influx upon prolonged supramaximal STIM2 signaling. This may explain an earlier finding that HEK293 cells with stably overexpressed STIM2 showed a similar inhibition (Soboloff et al., 2006a).

Synergistic regulation of Ca^{2+} influx by STIM1 and STIM2

While these experiments suggested that STIM1 and STIM2 can act independently of each other in regulating Ca^{2+} influx, we tested if they can also act synergistically by co-expression of STIM1 and STIM2 and their constitutively active mutants and using basal Ca^{2+} as a readout (Figure 6A). The observed higher basal Ca2+ levels in cells that express both constitutively active isoforms argues that STIM1 and STIM2 can synergize their activity when both isoforms are activated by lowering of ER Ca2+ concentration.

We further investigated the synergism and independent activation between STIM1 and STIM2 by imaging cells that had been co-transfected with wildtype CFP-STIM2 and constitutively active YFP-$STIM1_{EF}$. Upon depletion of ER Ca^{2+} stores, STIM2 translocated to the existing $STIM1_{EF}$ puncta while the localization of $STIM1_{EF}$ did not change (Figure 6B). In the reciprocal experiment, transfecting CFP-STIM1 and YFP-$STIM2_{EF}$ showed similar results with $STIM2_{EF}$ being prelocalized to puncta and STIM1 translocating to the puncta upon store depletion.

These results support the conclusion that STIM1 and STIM2 can act synergistically if both are activated when Ca^{2+} stores are depleted by strong receptor stimuli and that STIM2 functions independently of STIM1 for basal ER Ca2+ levels or weak receptor stimuli (Figure 6D).

Discussion

STIM2 regulates basal cytosolic and ER Ca^{2+} levels

Our study shows that STIM2 functions as a feedback regulator that stabilizes basal cytosolic and ER Ca^{2+} concentrations. This conclusion is based on the finding that STIM2 knockdown reduced basal and ER Ca^{2+} levels (Figure 2A–C) while STIM2 over-expression increased basal Ca^{2+} levels (Figure 2D). In contrast, STIM1 had only minimal effects on basal ER and cytosolic Ca2+ concentration.

Despite these differences between STIM2 and STIM1, important steps in the activation of STIM2 were similar to that of STIM1. STIM2 translocates to ER-PM junctions upon ER Ca^{2+}-store depletion (Figure 3A–E) and Orai1 knockdown sharply reduced the amplitude of the Ca^{2+} influx caused by STIM2 expression (Figure 3F). We also found that EF-hand mutants of STIM2 (deficient in Ca^{2+} binding) were no longer sensitive to ER Ca^{2+} concentration and were prelocalized to ER-PM junctions. This argues that STIM2, like STIM1, senses ER-Ca2 + levels, translocates to ER-PM junctions and regulates Orai1 PM Ca2+ channels.

We further found that while both STIM isoforms sense ER Ca^{2+} through their luminal EF-hand domain, the key difference is that STIM2 has a lower ER Ca^{2+} sensitivity than STIM1. Indeed, we found that STIM2 translocates to ER-PM junctions at a higher ER Ca^{2+} concentration compared to STIM1 (Figure 4A–C). This was supported by the finding that a STIM1 EF-hand switch of three amino acids from STIM1 to STIM2 created a STIM1 mutant with a lower Ca2+ sensitivity comparable to that of STIM2 (Figure S6C,D, S7). We also showed that STIM2 is partially active at basal ER Ca^{2+} levels and becomes more active once ER Ca^{2+} levels decline (Figure 4C). Markedly, this basal tuning point is near the linear range of STIM2 activation and can therefore provide cells with smooth homeostatic regulation rather than a switch like ON/OFF Ca^{2+} influx behavior. Finally, the surprisingly strong cooperativity in the Ca^{2+} dependence of STIM1 translocation provides for a potent mechanism that prevents STIM1 from being activated at basal ER Ca^{2+} concentrations. Together, these findings provide a molecular basis for the selective role of STIM2 in regulation basal Ca2+ concentration.

A STIM2-Orai1 control module tightly limits basal cytosolic and ER Ca^{2+} concentration

The long-term control of cytosolic Ca^{2+} levels is a function of the extracellular Ca^{2+} concentration and the balance between Ca^{2+} extrusion and Ca^{2+} influx at the plasma membrane. In turn, the long-term control of ER Ca^{2+} concentration is a function of cytosolic Ca^{2+} and the balance between Ca^{2+} pumping into the ER and Ca^{2+} flux out of the ER. If there would be no link between ER loading level and Ca^{2+} influx, deviations in basal Ca^{2+} concentration from normal caused by inadvertent cell stimuli or noise in gene expression would lead to harmful changes in ER Ca^{2+} concentration and cause ER stress. By using STIM2 to directly link basal ER Ca^{2+} levels to Ca^{2+} influx, cells can stabilize both cytosolic and ER Ca^{2+} concentration using a single feedback loop (Figure 7).

Thus, STIM2-mediated regulation of basal Ca^{2+} is relevant for cell function in multiple ways. By having sufficient cytosolic and ER Ca^{2+}, cells retain their ability to signal in response to receptor stimuli. By preventing excessive ER and cytosolic Ca^{2+} levels, cells reduce the likelihood for inadvertent activation of the signaling system. Indeed, as pointed out in the introduction, defective basal Ca^{2+} signaling has been linked to mitochondria dysfunction and ER-stress that can both be a secondary result of basal Ca^{2+} deregulation. In addition, different

proteases and many transcription factors are Ca^{2+} sensitive, and changes in basal Ca^{2+} levels can directly induce changes in cell state. Together, this argues that STIM2-mediated feedback stabilization of basal ER and cytosolic Ca^{2+} levels serves as an important support mechanism for the long term health of cells.

Role of STIM2 in triggering persistent Ca2+ increases in response to submaximal receptor stimuli

We found that STIM2, like STIM1, can activate R-SOC type Ca^{2+} influx when Ca^{2+} stores are maximally depleted. The activation of Orai1 by STIM2 was independent of STIM1 (Figure 5A,B), suggesting that STIM2 can act alone or in conjunction with STIM1 to trigger R-SOC. Such a role of STIM2 in R-SOC is also consistent with our previous identification of STIM2 as a weak yet significant hit in a siRNA screen to identify regulators of store-depletion activated Ca^{2+} influx (Liou et al., 2005).

Since our study showed that STIM2 can be readily activated by submaximal reductions in ER Ca2+, it is likely that STIM2 has also a unique role in triggering persistent Ca^{2+} increases in response to submaximal receptor stimuli. It is therefore likely that STIM2 has two roles: First, to serve as a stabilizer of basal Ca^{2+} and, second, as a more sensitive regulator of R-SOC compared to STIM1 that can selectively open PM Ca^{2+} channels for submaximal receptor stimuli.

Evolution from a single STIM protein to a dual STIM1, STIM2 system

Given that *Drosophila melanogaster* has a single ubiquitously expressed STIM protein, we speculate that STIM proteins had an ancestral role reminiscent of STIM2 in regulating basal ER and cytosolic Ca^{2+} concentrations. This stabilization function may initially have been more important than its role in receptor-triggered Ca2+ signaling. Gene duplication in vertebrates may have enabled a dual use of STIM proteins, with a less sensitive STIM2 version that functions as a regulator of basal Ca^{2+} and a mediator of persistent Ca2+ increases for weak receptor stimuli. In contrast, the more sensitive STIM1 version became specialized to mediate persistent Ca^{2+} increases for strong receptor stimuli.

In summary, our study identified STIM2 in a siRNA screen of the human signaling proteome as the strongest positive regulator of basal cytosolic Ca^{2+} concentration. In contrast to STIM1, a recently identified signaling mediator that triggers Ca^{2+}-influx in response to receptor-mediated Ca^{2+} release, STIM2 is active at basal ER Ca^{2+} concentrations and can be further activated by small reductions in ER Ca^{2+}. Together, this defines a STIM2-Orai1 feedback module that keeps basal cytosolic as well as ER Ca^{2+} concentrations within a narrow range.

Materials and Methods

Cell Transfection, Plasmids, and Reagents

STIM1 and STIIM2 synthetic siRNA were purchased from Ambion and Dharmacon, respectively. Diced siRNA against GL3 luciferase was used as a transfection control. HeLa, HUVEC, and HEK293T cells were purchased from ATCC. DNA plasmids were transfected with Fugene 6 reagent (Roche). siRNA was transfected with Gene Silencer (Gene Therapy Systems) for HeLa, Lipofectamine 2000 (Invitrogen) for HEK293T, and Lipofectin (Invitrogen) for HUVEC. Full-length human STIM1 and STIM2 cDNA were isolated by PCR, sequenced, and cloned in to pDS_XB-YFP vector (ATCC). See Figure S9 for details on constructs. Briefly, the YFP-conjugated EF-hand mutants of STIM1, $STIM1_{EF}$(D76A), and STIM2, $STIM2_{EF}$(D80A), $STIM2_{EF->STIM1}$ (K83A, D84N, G86D), $STIM1_{EF->STIM2}$ (A79K, N80D, D82G) were made by site-directed mutagenesis with the QuikChange Site-Directed Mutagenesis Kit (Stratagene). Thapsigargin (Invitrogen) and ionomycin (Sigma) and BHQ

(EMD Bioscience) were used at 1 μM. Antibodies purchased from Prosci (STIM1, STIM2) and AbCam (GAPDH).

siRNA Library of Signaling Proteins

The synthesis of the Dicer generated siRNA library was described previously (Liou et al., 2005). In short, siRNAs were made targeting 2304 human signaling-related proteins selected from the NCBI (RefSeq database) on the basis of the presence of signaling domains, such as protein kinase, SH2, SAM, EF, and PH domains, as well as by text searches of signaling-related terms.

Ca^{2+} Measurements

HeLa cells were loaded with 1 μM Fura-2-AM in extracellular buffer (125 mM NaCl, 5 mM KCl, 1.5 mM $MgCl_2$, 20 mM HEPES, 10 mM glucose, and 0.1, 1.5, 11.8 mM $CaCl_2$ [pH 7.4]) for 30 min at room temperature. Fura-2 fluorescence was measured by exciting Fura-2 using alternating 340/380 nm illumination and measuring fluorescence intensity at 510 nm. Intracellular Ca^{2+} concentration was computed from the ratio of fluorescence intensity for excitation at 340 and 380 nm. For the RNAi screen, the values for each well of the 384 well plate have been subject to two normalization steps. First, regional background subtraction was performed between neighboring wells to correct for trends across the well plate. Second, the values are presented as fold standard deviations from the median of the screen. For all other figures, Fura-2 ratio was calibrated using:

$$[Ca^{2+}]=Kd^{*}Q^{*}(R-Rmin)/(Rmax-R),\text{where } Kd=0.14\,\mu M$$

R_{max} was determined by measuring the maximal attainable fluorescence intensity in cells treated with ionomycin in high external Ca^{2+} (R_{max}= 6.06). R_{min} and Q values are dependent on autofluorescence, unspecific Fura-2 binding to cellular components as well as on Fura-2 sequestration inside cells. We adjusted them for HeLa cells so that the average basal Ca^{2+} level was 50 nM in calibration experiments (R_{min}= 0.217 and Q = 9.71). The same R_{max}, R_{min} and Q values were used for all experiments shown. However, experiments that took a longer time to image required a final offset of −20 nM s due to presumed dye loading into stores.

For Ca^{2+} add-back experiments, 3 mM EGTA was added together with thapsigargin to remove extracellular Ca^{2+}, and extracellular Ca^{2+} was changed to a final Ca^{2+} concentration of 0.75 mM 15 minutes later. Imaging-based single-cell Ca^{2+} measurements were performed with a 4x objective on an automated fluorescent microscope (ImageXpress 5000A, Molecular Devices). Fluorescence intensities of single cells were calculated using Matlab 7.1 software.

Extracellular Ca^{2+} manipulation

For the RNAi screen, low Ca^{2+} conditions were created by replacing normal media (Dulbecco's Modified Eagle's Medium (DMEM), 10% fetal bovine serum, penicillin, streptomycin, glutamate) with media made using DMEM without Ca^{2+} (Invitrogen). For other experiments, low Ca^{2+} media was created by adding 2 mM EGTA to normal media. High extracellular Ca^{2+} media was made by adding 10 mM Ca^{2+} to normal media.

Puncta Analysis

Puncta analysis for STIM1 and STIM2 translocation were performed by applying a bandpass filter and then taking the mean of the square of the pixels in the resulting image. Each time-series of values was then linearly transformed to range between 0 and 1.

FRET Imaging

CFP and FRET images were first background subtracted. The average FRET/CFP per pixel was computed for a mask created using the CFP channel. For Figure 2C, a 4x objective and EPI-fluorescence microscope was used to collect data from thousands of cells. For Figure S6, a 40x objective was used to most accurately measure change in FRET/CFP after EGTA for single cells.

Western Blot Conditions

Primary antibodies were used at 1:1000 dilution and 17.5 μg of protein samples/lane run on a 4–12% tris-glycine gel. Cells were lysed in modified RIPA buffer (specified below) and then spun down for 45 minutes to remove membranes. Samples were boiled for 5 minutes after addition of sample buffer.

Lysis buffer: 150 mM NaCl, 50 mM Tris-HCl (pH 7.4),1 mM EDT, 1% Triton X-100, 1% sodium deoxycholic acid, 0.1% SDS, 1 mM PMSF, 5 μg/ml aprotinin, 5 μg/ml leupeptin.

Supplementary Material

Refer to Web version on PubMed Central for supplementary material.

Acknowledgements

We thank the following people for contributions: Phil Vitorino, Mark Hammer and Dr. Marc Fivaz for helpful suggestions and careful reading of the manuscript. Drs. Rajat Rohatgi and Eric Humke for help with Western blots. Dr. Yigal Brandman for help with puncta analysis. Man Lyang Kim and Drs. Won Do Heo, Josh Jones, and Jason Myers for generating the siRNA library and JL. Jess Field for help with graphic design. This work was supported by a grant to TM from the Sandler Foundation and NIH grant GM030179. OB was funded by an NSF Predoctoral Fellowship.

References

Berridge MJ, Bootman MD, Roderick HL. Ca^{2+} signalling: dynamics, homeostasis and remodelling. Nat Rev Mol Cell Biol 2003;4:517–29. [PubMed: 12838335]

Bezprozvanny I, Hayden MR. Deranged neuronal Ca^{2+} signaling and Huntington disease. Biochem Biophys Res Commun 2004;322:1310–7. [PubMed: 15336977]

Brini M, Pinton P, Pozzan T, Rizzuto R. Targeted recombinant aequorins: tools for monitoring [Ca^{2+}] in the various compartments of a living cell. Microsc Res Tech 1999;46:380–9. [PubMed: 10504215]

Camello C, Lomax R, Petersen OH, Tepikin AV. Calcium leak from intracellular stores--the enigma of calcium signalling. Cell Calcium 2002;32:355–61. [PubMed: 12543095]

Campanella M, Pinton P, Rizzuto R. Mitochondrial Ca^{2+} homeostasis in health and disease. Biol Res 2004;37:653–60. [PubMed: 15709694]

Dziadek MA, Johnstone LS. Biochemical properties and cellular localisation of STIM proteins. Cell Calcium. 2007(epub Mar 21)

Feske S, Gwack Y, Prakriya M, Srikanth S, Puppel SH, Tanasa B, Hogan PG, Lewis RS, Daly M, Rao A. A mutation in ORAI1 causes immune deficiency by abrogating CRAC channel function. Nature 2006;441:179–85. [PubMed: 16582901]

Grynkiewicz G, Poenie M, Tsien RY. A new generation of Ca^{2+} indicators with greatly improved fluorescence properties. J Biol Chem 1985;260:3440–50. [PubMed: 3838314]

Guerini D, Coletto L, Carafoli E. Exporting Ca^{2+} from cells. Cell Calcium 2005;38:281–9. [PubMed: 16102821]

Kusters JM, Dernison MM, van Meerwijk WP, Ypey DL, Theuvenet AP, Gielen CC. Stabilizing role of calcium store-dependent plasma membrane calcium channels in action-potential firing and intracellular calcium oscillations. Biophys J 2005;89:3741–56. [PubMed: 16169971]

Liou J, Fivaz M, Inoue T, Meyer T. Live-cell imaging reveals sequential oligomerization and local plasma membrane targeting of stromal interaction molecule 1 after Ca^{2+} store depletion. Proc Natl Acad Sci U S A 2007;104:9301–6. [PubMed: 17517596]

Liou J, KimMLHeo WD, Jones JT, Myers JW, Ferrell JE Jr, Meyer T. STIM is a Ca^{2+} sensor essential for Ca^{2+}-store-depletion-triggered Ca^{2+} influx. Curr Biol 2005;15:1235–41. [PubMed: 16005298]

Luik RM, Wu MM, Buchanan J, Lewis RS. The elementary unit of store-operated Ca^{2+} entry: local activation of CRAC channels by STIM1 at ER-plasma membrane junctions. J Cell Biol 2006;174:815–25. [PubMed: 16966423]

Mercer JC, Dehaven WI, Smyth JT, Wedel B, Boyles RR, Bird GS, Putney JW Jr. Large store-operated Ca^{2+} selective currents due to co-expression of ORAI1 or ORAI2 with the intracellular Ca^{2+} sensor, STIM1. J Biol Chem 2006;281:24979–90. [PubMed: 16807233]

Montero M, Barrero MJ, Torrecilla F, Lobaton CD, Moreno A, Alvarez J. Stimulation by thimerosal of histamine-induced Ca(2+) release in intact HeLa cells seen with aequorin targeted to the endoplasmic reticulum. Cell Calcium 2001 Sep;30(3):181–90. [PubMed: 11508997]

Myers JW, Jones JT, Meyer T, Ferrell JE Jr. Recombinant Dicer efficiently converts large dsRNAs into siRNAs suitable for gene silencing. Nat Biotechnol 2003;21:324–8. [PubMed: 12592410]

Palmer AE, Jin C, Reed JC, Tsien RY. Bcl-2-mediated alterations in endoplasmic reticulum Ca^{2+} analyzed with an improved genetically encoded fluorescent sensor. Proc Natl Acad Sci U S A 2004 Dec 14;101(50):17404–9. [PubMed: 15585581]

Peinelt C, Vig M, Koomoa DL, Beck A, Nadler MJ, Koblan-Huberson M, Lis A, Fleig A, Penner R, Kinet JP. Amplification of CRAC current by STIM1 and CRACM1 (ORAI1). Nat Cell Biol 2006;8:771–3. [PubMed: 16733527]

Periasamy M, Kalyanasundaram A. SERCA pump isoforms: their role in calcium transport and disease. Muscle Nerve 2007;35:430–42. [PubMed: 17286271]

Philipson KD, Nicoll DA, Ottolia M, Quednau BD, Reuter H, John S, Qiu Z. The Na+/Ca^{2+} exchange molecule: an overview. Ann N Y Acad Sci 2002;976:1–10. [PubMed: 12502528]

Pinton P, Rizzuto R. Bcl-2 and Ca^{2+} homeostasis in the endoplasmic reticulum. Cell Death Differ 2006;13:1409–18. [PubMed: 16729032]

Raza M, Deshpande LS, Blair RE, Carter DS, Sombati S, Delorenzo RJ. Aging is associated with elevated intracellular Ca^{2+} levels and altered Ca^{2+} homeostatic mechanisms in hippocampal neurons. Neurosci Lett 2007;418:77–81. [PubMed: 17374449]

Roos J, DiGregorio PJ, Yeromin AV, Ohlsen K, Lioudyno M, Zhang S, Safrina O, Kozak JA, Wagner SL, Cahalan MD, Velicelebi G, Stauderman KA. STIM1, an essential and conserved component of store-operated Ca^{2+} channel function. J Cell Biol 2005;169:435–45. [PubMed: 15866891]

Schulman IH, Zachariah M, Raij L. Ca^{2+} channel blockers, endothelial dysfunction, and combination therapy. Clin Exp Res 2005;17:40–5.

Soboloff J, Spassova MA, Hewavitharana T, He LP, Xu W, Johnstone LS, Dziadek MA, Gill DL. STIM2 is an inhibitor of STIM1-mediated store-operated Ca^{2+} Entry. Curr Biol 2006a;16:1465–70. [PubMed: 16860747]

Soboloff J, Spassova MA, Tang XD, Hewavitharana T, Xu W, Gill DL. ORAI1 and STIM reconstitute store-operated Ca^{2+} channel function. J Biol Chem 2006b;281:20661–5. [PubMed: 16766533]

Spira ME, Oren R, Dormann A, Ilouz N, Lev S. Calcium, protease activation, and cytoskeleton remodeling underlie growth cone formation and neuronal regeneration. Cell Mol Neurobiol 2001;21:591–604. [PubMed: 12043835]

Stathopulos PB, Li GY, Plevin MJ, Ames JB, Ikura M. Stored Ca^{2+} depletion-induced oligomerization of stromal interaction molecule 1 (STIM1) via the EF-SAM region: An initiation mechanism for capacitive Ca^{2+} entry. J Biol Chem 2006;281:35855–62. [PubMed: 17020874]

Strehler EE, Caride AJ, Filoteo AG, Xiong Y, Penniston JT, Enyedi A. Plasma membrane Ca^{2+} ATPases as dynamic regulators of cellular calcium handling. Ann N Y Acad Sci 2007;1099:226–36. [PubMed: 17446463]

Ter Keurs HE, Boyden PA. Ca^{2+} and arrhythmogenesis. Physiol Rev 2007;87:457–506. [PubMed: 17429038]

Thastrup O, Cullen PJ, Drobak BK, Hanley MR, Dawson AP. Thapsigargin, a tumor promoter, discharges intracellular Ca^{2+} stores by specific inhibition of the endoplasmic reticulum Ca2(+)-ATPase. Proc Natl Acad Sci U S A 1990;87:2466–70. [PubMed: 2138778]

Thebault S, Hoenderop JG, Bindels RJ. Epithelial Ca^{2+} and Mg^{2+} channels in kidney disease. Adv Chronic Kidney Dis 2006;13:110–7. [PubMed: 16580611]

Treves S, Anderson AA, Ducreux S, Divet A, Bleunven C, Grasso C, Paesante S, Zorzato F. Ryanodine receptor 1 mutations, dysregulation of Ca^{2+} homeostasis and neuromuscular disorders. Neuromuscul Disord 2005;15:577–87. [PubMed: 16084090]

Tu H, Nelson O, Bezprozvanny A, Wang Z, Lee SF, Hao YH, Serneels L, De Strooper B, Yu G, Bezprozvanny I. Presenilins form ER Ca^{2+} leak channels, a function disrupted by familial Alzheimer's disease-linked mutations. Cell 2006;126:981–93. [PubMed: 16959576]

Wu MM, Buchanan J, Luik RM, Lewis RS. Ca^{2+} store depletion causes STIM1 to accumulate in ER regions closely associated with the plasma membrane. J Cell Biol 2006;174:803–13. [PubMed: 16966422]

Yeromin AV, Zhang SL, Jiang W, Yu Y, Safrina O, Cahalan MD. Molecular identification of the CRAC channel by altered ion selectivity in a mutant of ORAI. Nature 2006;443:226–9. [PubMed: 16921385]

Yu R, Hinkle PM. Rapid turnover of calcium in the endoplasmic reticulum during signaling. Studies with cameleon calcium indicators. J Biol Chem 2000;275:23648–53. [PubMed: 10811650]

Zhang K, Kaufman RJ. The unfolded protein response: a stress signaling pathway critical for health and disease. Neurology 2006;66:S102–9. [PubMed: 16432136]

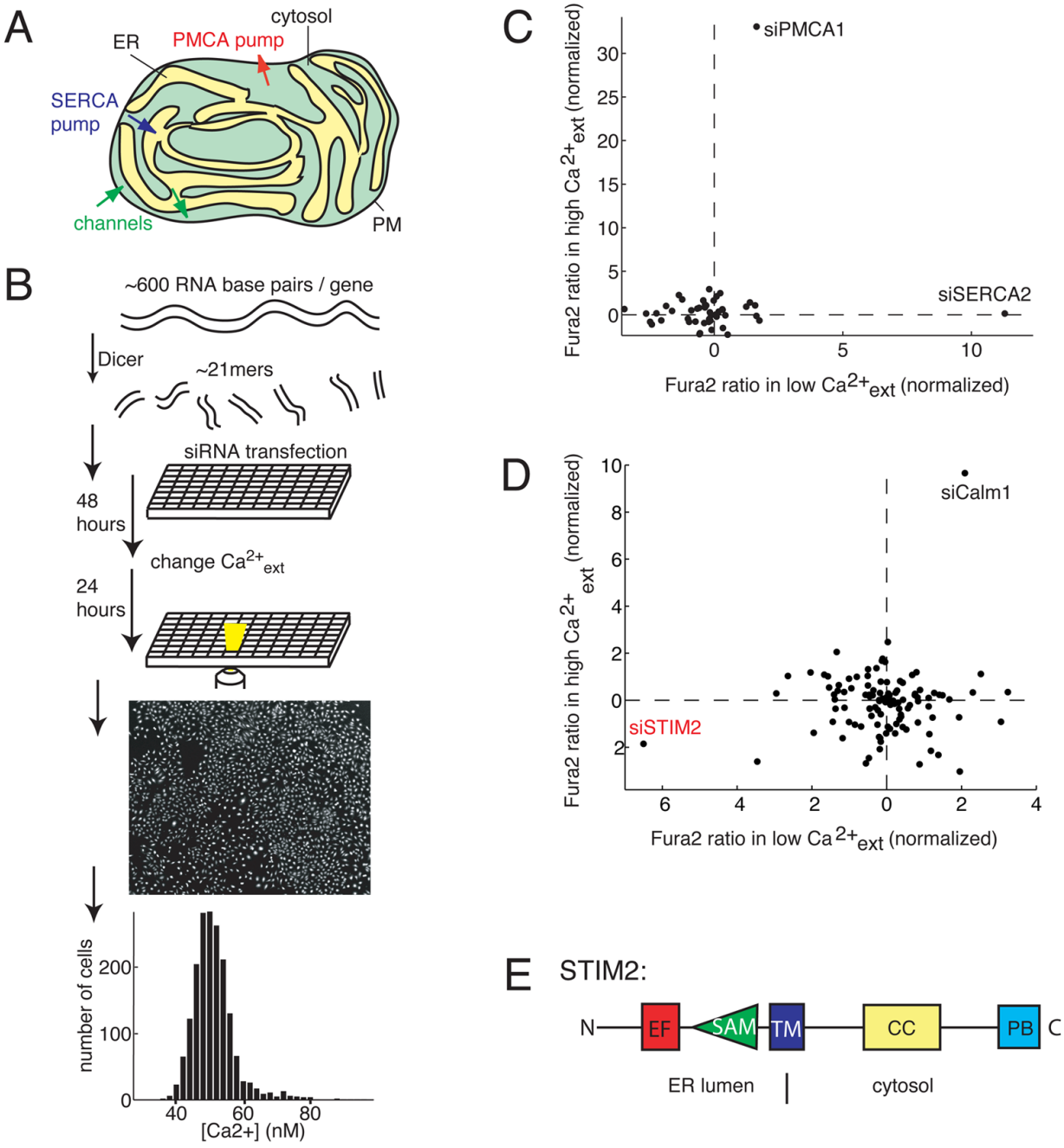

Figure 1. Identification of STIM2 as a regulator of basal Ca^{2+} concentration

(A) Overview of intracellular Ca^{2+} homeostasis. Basal cytosolic Ca^{2+} concentration is controlled by PM as well as ER Ca^{2+} channels and pumps.

(B) Sensitized siRNA screening assay for basal Ca^{2+} regulation. 2304 diced siRNA constructs were individually transfected into HeLa cells and cultured in 384 well plates. High and Low extracellular Ca^{2+} exposure (+10 mM and ~0.1 mM) were used for sensitization. Single cell Ca^{2+} levels were measured using automated image analysis software.

(C) Test experiments using a siRNA set targeting Ca^{2+} pumps, channels, and exchangers (performed in duplicate). Deviations from control Ca^{2+} levels are shown in units of standard deviation.

(D) Result from the sensitized siRNA screen of the human signaling proteome highlighting STIM2 and Calm1 as primary hits (performed in triplicate).
(E) Schematic representation of modular domains found in STIM2. On the luminal side: EF-hand is a Ca^{2+} binding domain and SAM is a conserved protein interaction domain. On the cytosolic side: CC and PB are a coiled-coil and a polybasic region, respectively.

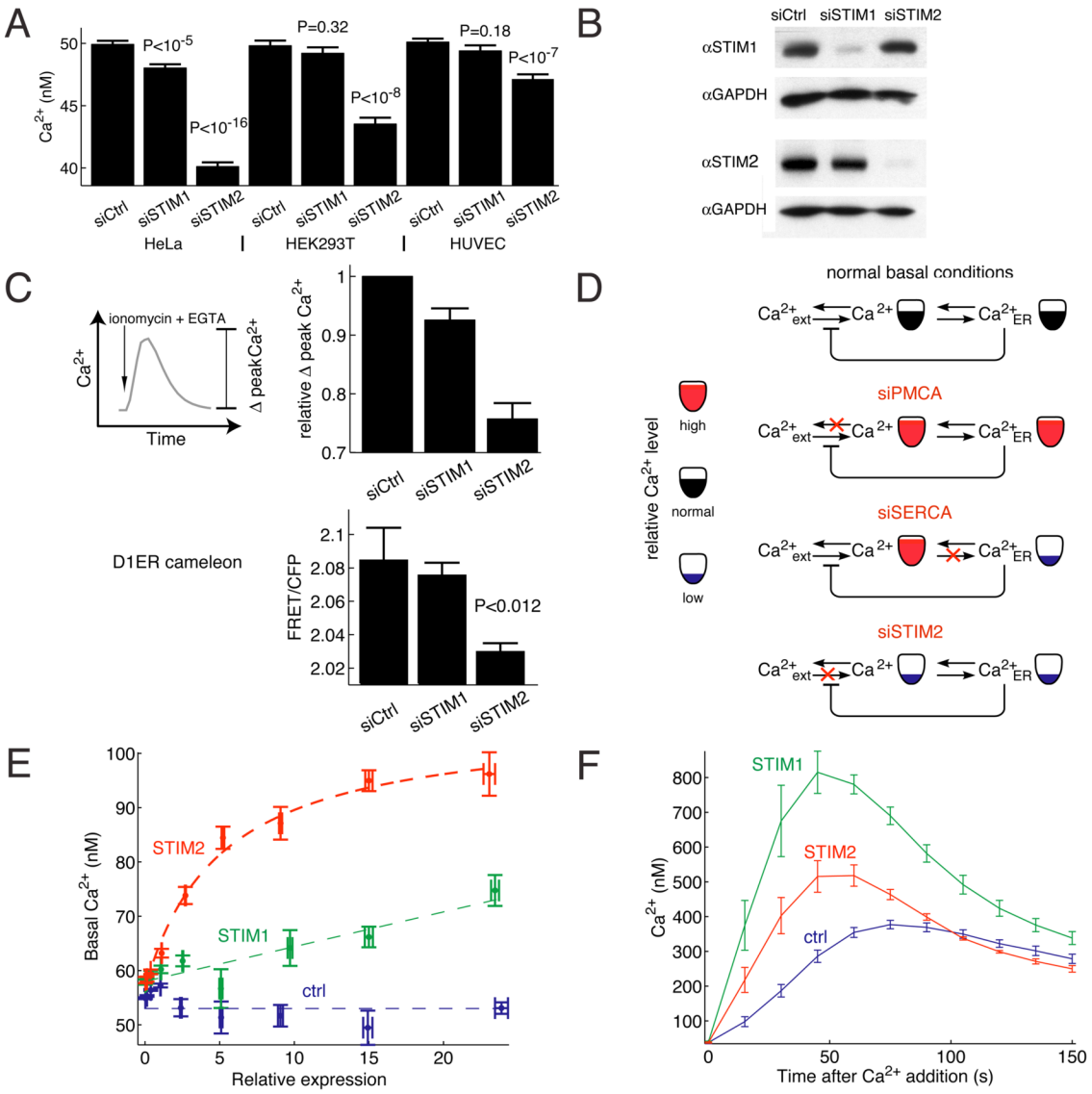

Figure 2. STIM2 controls basal cytosolic and ER Ca^{2+} concentration

(A) Comparison of basal Ca^{2+} levels after siRNA knockdown of STIM2 compared to STIM1. HeLa, HUVEC, and HEK293T cells were transfected with synthetic siRNA against STIM2 and STIM1 as well as diced GL3 as a control. N=10 sites; error bars represent standard error.

(B) STIM1 and STIM2 siRNA specificity assayed by Western blot. HeLa cells were tranfected with siRNAs targeting STIM1, STIM2 or control for 3 days.

(C) STIM2 knockdown lowers basal ER Ca^{2+}. ER Ca^{2+} levels were measured in two ways. First, as the Ca^{2+} pool released by addition of the Ca^{2+}-ionophore ionomycin. 1 μM ionomycin + 3 mM EGTA were added to HeLa cells and the increase in cytosolic Ca^{2+} was measured (Δpeak). Single cell analysis from 3 wells each. In a second method, the ER targeted cameleon D1ER was transfected into cells two days after siRNA transfection and one day before imaging. FRET/CFP was then computed as described in Materials and Methods (8 sites).

(D) Schematic representation of the effects of PMCA1, SERCA2, and STIM2 knockdowns on basal Ca^{2+} levels in the ER and cytosol.

(E) Single cell analysis of basal Ca^{2+} concentration as a function of the expression level of YFP-STIM2 versus YFP-STIM1. Cells were transfected for 9 hours with YFP-STIM1, YFP-STIM2, or YFP (as a control). Ca^{2+} levels and YFP construct expression were measured for each cell. YFP fluorescence was normalized to the background in the YFP channel.
(F) Single cell analysis of Ca^{2+}-influx triggered by ER Ca^{2+} store-depletion (Ca^{2+}-add back experiments). Cells were depleted of ER Ca^{2+} by additions of 1 μM thapsigargin to block SERCA pumps and 3 mM external EGTA to prevent Ca^{2+} influx. Ca^{2+} was added back (to a free concentration of 0.75 mM) at t=0 to measure Ca^{2+} influx rates. Single cells were analyzed in 3 independent wells for each condition.

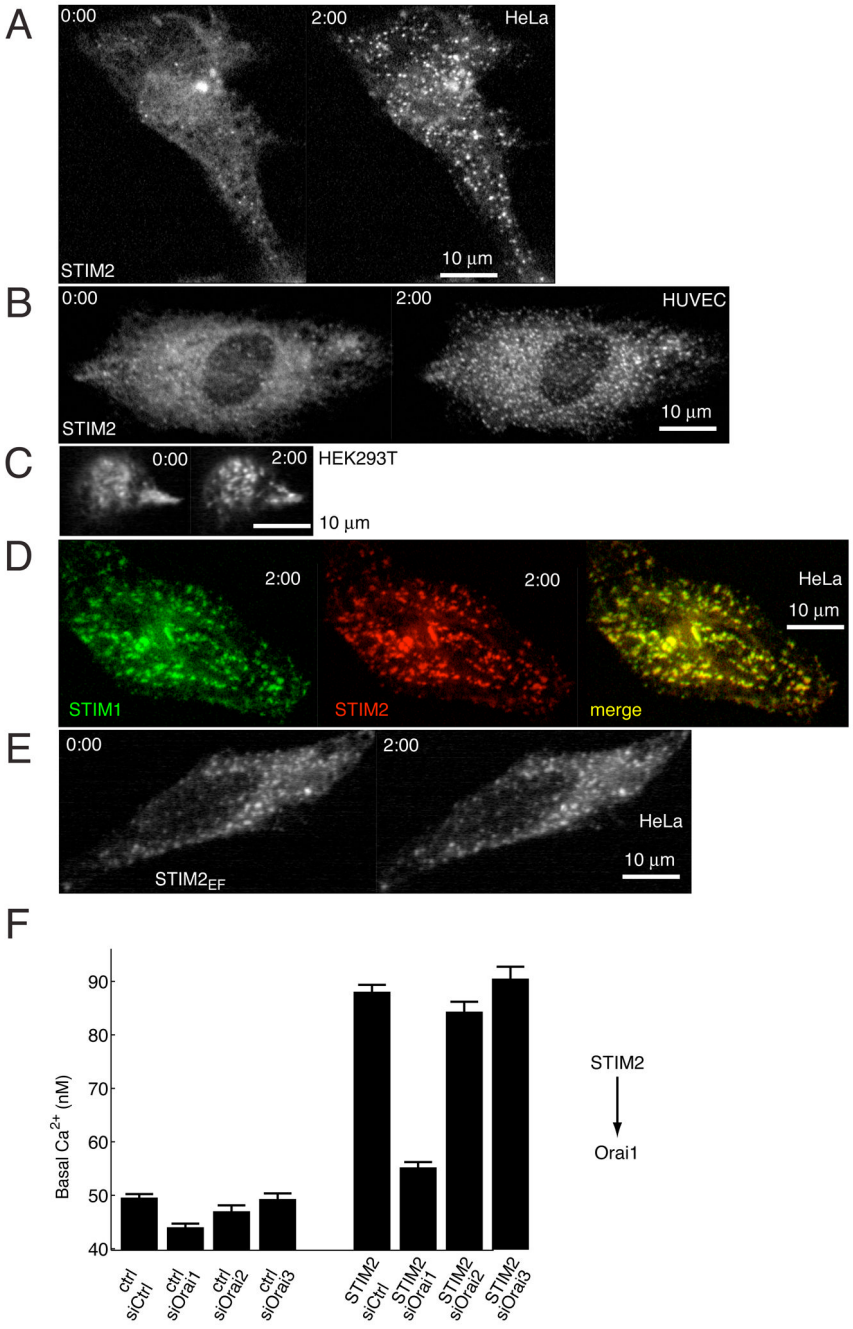

Figure 3. STIM2 translocates to ER-PM junctions following ER Ca^{2+} depletion and regulates Orai1

(A–C) YFP-STIM2 was expressed (~24 hour) in HeLa (A), HUVEC, (B), and HEK293T (C) cells and confocal images were taken before and 2 minutes after 1 µM thapsigargin addition.

(D) Comparison of the distribution of CFP-STIM1 and YFP-STIM2 constructs 2 min after addition of thapsigargin.

(E) Ca^{2+}-binding deficient YFP-STIM2 (point mutation in EF-hand) is prelocalized to ER-PM junction sites and does not alter its localization after Ca^{2+} store depletion.

(F) Knockdown of the PM Ca^{2+} channel Orai1 significantly reduces the increase in basal Ca^{2+} resulting from STIM2 expression. HeLa cells were transfected for two days with GL3, Orai1, Orai1, or Orai3 siRNA and then transfected for 24 hours with YFP-STIM2 or YFP as

control. Cells used in the analysis expressed YFP at 7.5 to 15 fold above background. N=10 sites.

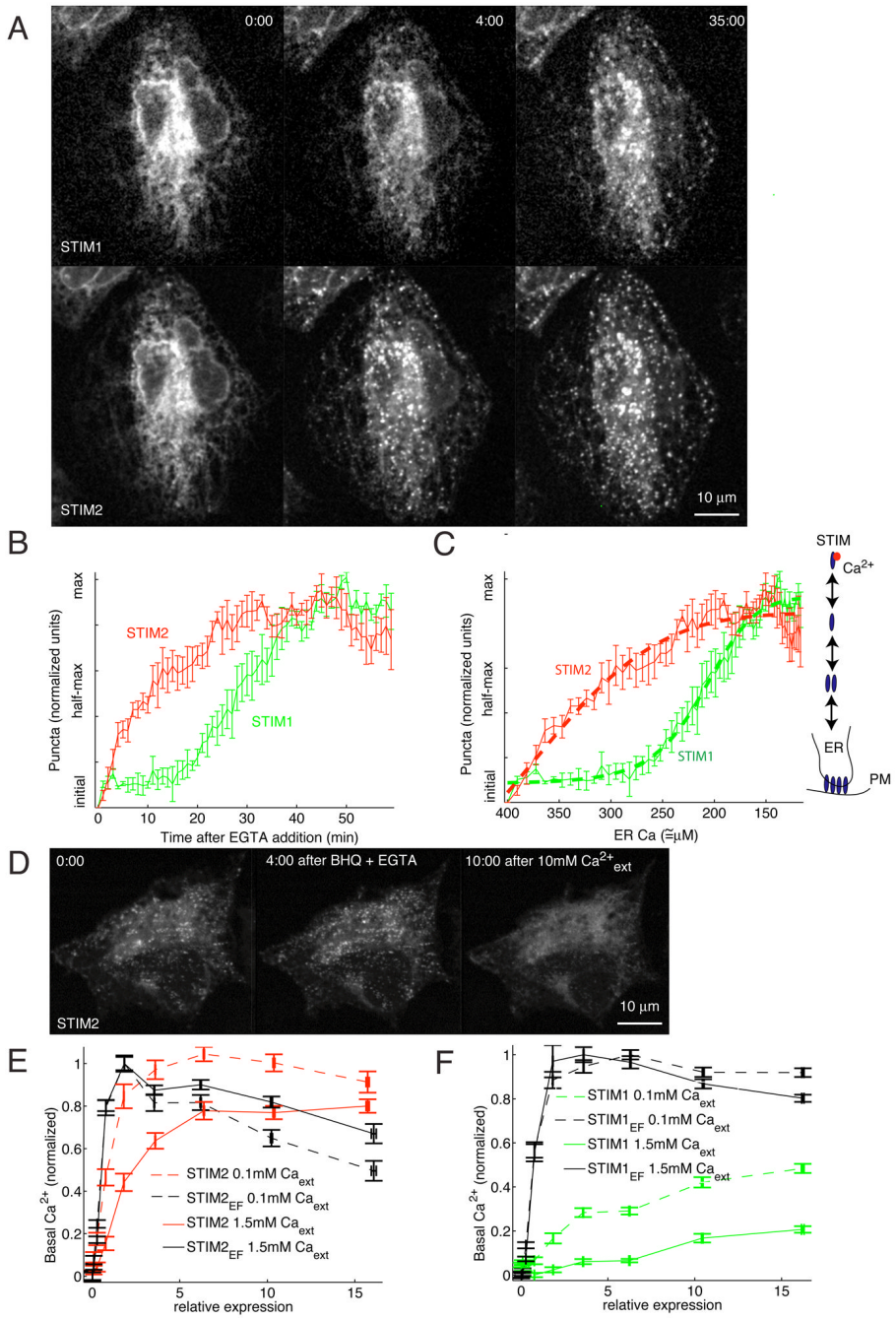

Figure 4. STIM2 translocation is cooperatively triggered by small decreases in ER Ca^{2+} concentration compared to larger decreases needed for STIM1

(A) STIM2 translocates to ER-PM junctions for small decreases in ER Ca^{2+} concentrations compared to STIM1. YFP-STIM2 and CFP-STIM1 were co-tranfected (~24 hour) and imaged in the same cells. ER Ca^{2+} stores were depleted slowly by extracellular addition of 3 mM EGTA. YFP-STIM2 and CFP-STIM1 distributions are compared before, 4 minutes after and 35 minutes after 3 mM EGTA addition.

(B) Analysis of the kinetics of STIM1 and STIM2 translocation to ER-PM junctions upon EGTA addition. 3 mM EGTA was added to HeLa cells and imaged for 60 minutes. Cells were

analyzed for puncta content as described in the Materials and Methods section. Average puncta intensity from N=5 cells.

(C) Calibration and quantitative model derived from the data in (B). ER Ca^{2+} concentration was calibrated as a function of time after EGTA addition (Figure S5A). The concentration dependence of translocation was then fit to a cooperative oligomerization and translocation model (thick dashed lines). The scheme shows the key features of our model that includes, in addition to the differential Ca^{2+} sensitivity, an oligomerization and translocation process with a cooperativity of 5 for STIM2 and 8 for STIM1 activation.

(D) ER Ca^{2+} overload reduces STIM2 puncta to sub-basal levels. 1 μM BHQ + 3 mM EGTA was added to YFP-STIM2 expressing cells and then washed out with extracellular buffer containing 10 mM Ca^{2+}, causing a large Ca^{2+} influx and super-normal ER Ca^{2+} levels.

(E-F) Functional comparison supporting that STIM2 activity is suppressed at higher ER-Ca^{2+} levels compared to STIM1. Basal Ca^{2+} levels were measured as a function of the expression level of STIM1 and STIM2 constructs (9 h of transfection). Normal (dashed lines) and reduced (solid lines) ER Ca^{2+} levels were used to probe for the STIM1 and STIM2 Ca^{2+} sensitivities. Expression of EF-hand mutant STIM2 and STIM1 constructs (black) were employed as a reference of Ca^{2+}-insensitive and constitutively active proteins and were used to normalize the wildtype data (each isoform of STIM was divided by the maximum basal level for the corresponding EF hand mutant in the same condition). In normal ER conditions, wildtype STIM1 (green) or STIM2 (red) expression showed a marked difference in basal Ca^{2+} profile compared the EF-hand mutants. In contrast, STIM2 but not STIM1 closely matched the profile of its EF-hand mutant at reduced ER Ca^{2+} levels, suggesting that reduced ER Ca^{2+} levels can still suppress STIM1 but not STIM2 activity. N=25 sites.

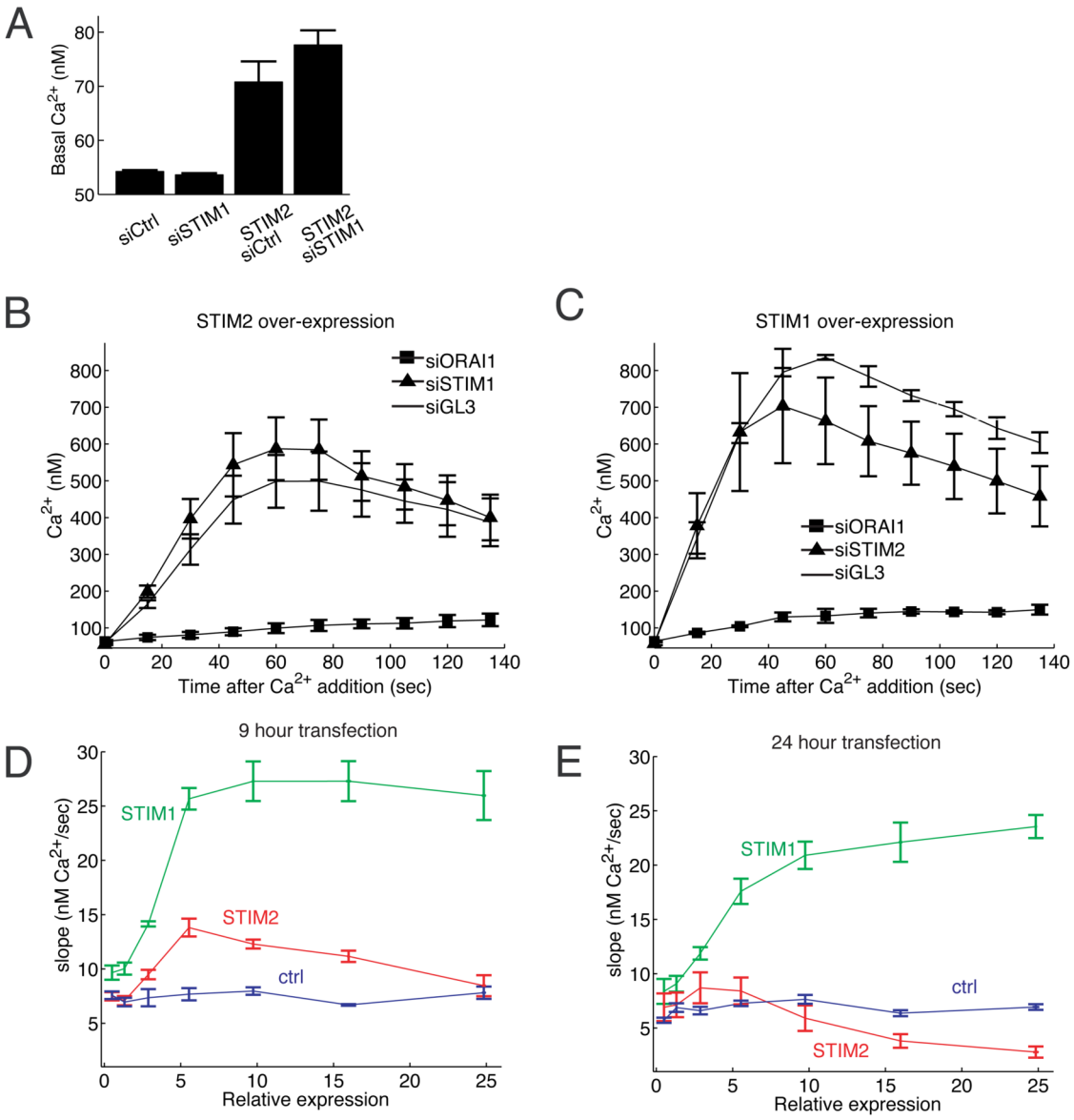

Figure 5. STIM2 can regulate Ca^{2+} influx independent of STIM1

(A) STIM2 expression-mediated increases in basal Ca^{2+} are not affected by knockdown of STIM1. Cells were transfected with YFP-STIM2 ~60 hours after STIM1 or GL3 control siRNA transfection and 9 hours before imaging. Cells selected expressing YFP at background autofluorescence (non transfected) or 4–8 times autofluorescense (transfected). N=15 sites.

(B-C) Experiments showing that STIM2-triggered R-SOC is not affected by STIM1 knockdown and STIM1-triggered R-SOC is not significantly affected by STIM2 knockdown. Ca^{2+} addback experiments were performed in cells prepared and selected as described in (A) expressing STIM2 (B) and STIM1 (C). 9 hour transfection. N=3 wells.

(D-E) Control experiment showing that prolonged overexpression of YFP-STIM2 downregulates the maximal attainable Ca^{2+} influx rate. Influx rates were measured in Ca^{2+} add-back experiments in the presence of thapsigargin. Expression at 9 hours (D) is compared to expression at 24 hours (E). N=4 sites from 2 wells.

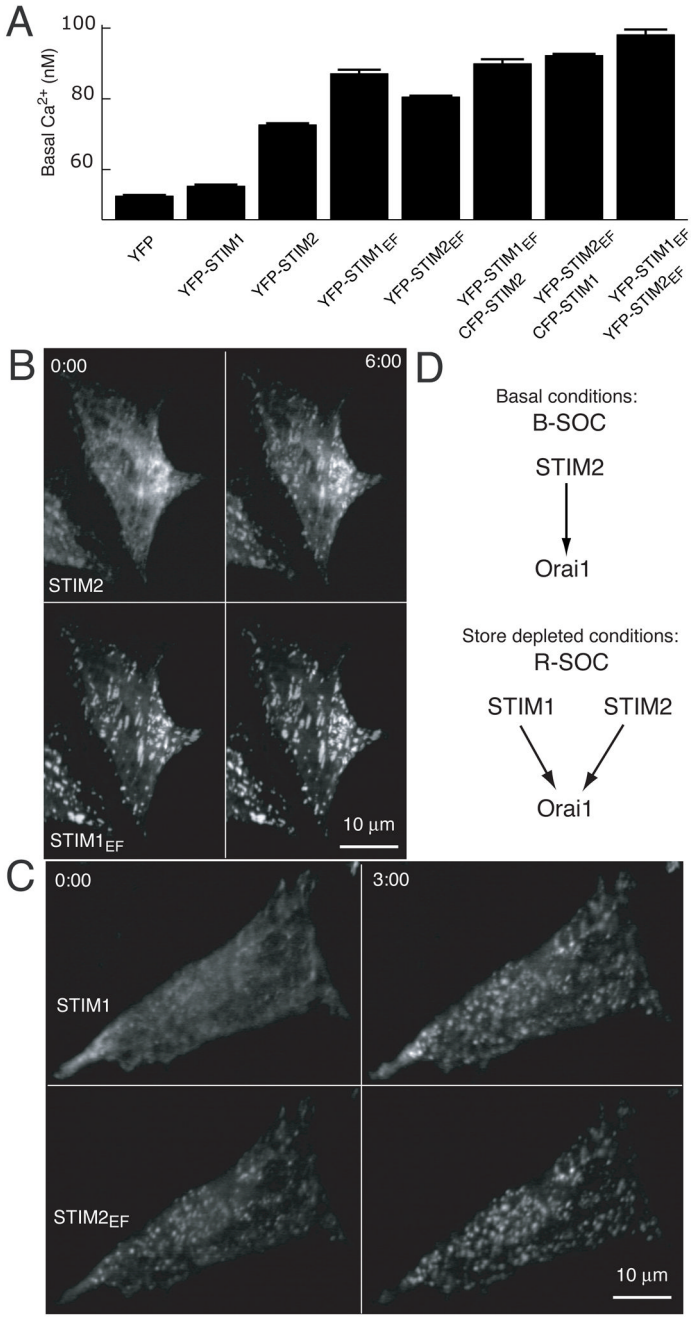

Figure 6. STIM2 and STIM1 act synergistically and independently of each other

(A) Test for synergism and independence between STIM1 and STIM2. YFP tagged constructs were cotransfected with YFP or CFP constructs as indicated for 24 hours. Ca^{2+}-levels are shown for cells expressing YFP signals 1–3 fold above autofluorescence.

(B) STIM2 can translocate in the presence of prelocalized $STIM1_{EF}$. CFP-STIM2 and YFP-$STIM1_{EF}$ were cotransfected and imaged before and 6 minutes after addition of 1 μM thapsigargin.

(C) STIM1 can translocate in the presence of of prelocalized $STIM2_{EF}$. CFP-STIM1 and YFP-$STIM2_{EF}$ were cotransfected and imaged before and 3 minutes after addition of 1 μM thapsigargin.

(D) Schematic representation of identified regulators of Ca^{2+}-influx for basal versus receptor-triggered stimulation condition.

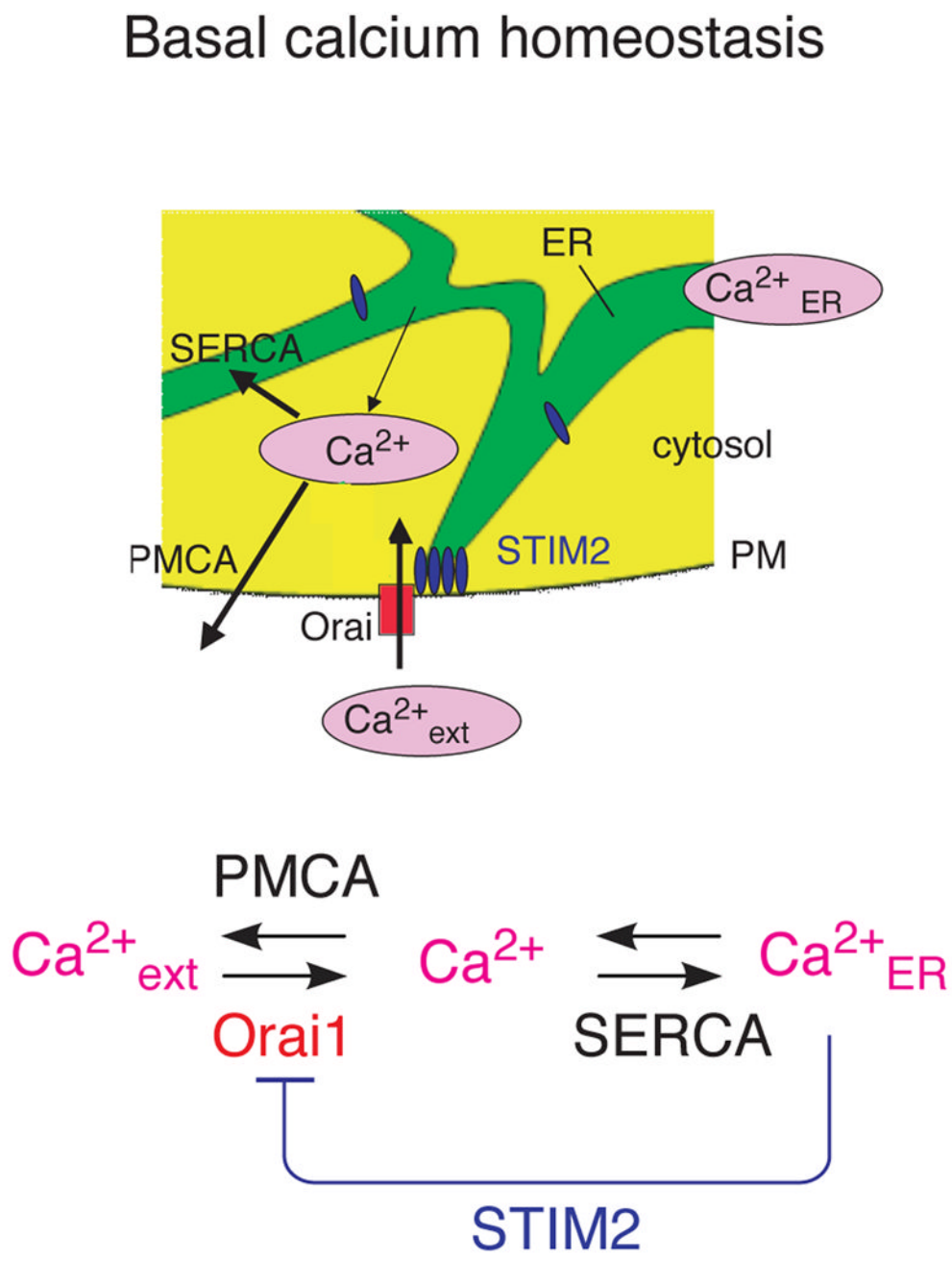

Figure 7. Model for STIM2 function in basal Ca^{2+} homoestasis

Schematic representations of the stabilization of basal cytosolic and ER Ca^{2+} concentrations by negative feedback.